

# Sulphur-bearing lipids for the covalent attachment of supported lipid bilayers to gold surfaces: a detailed characterisation and analysis

Claus Duschl<sup>a,\*</sup>, Martha Liley<sup>a</sup>, Holger Lang<sup>a</sup>, Azin Ghandi<sup>a</sup>, Shaik M. Zakeeruddin<sup>b</sup>,  
Henning Stahlberg<sup>c</sup>, Jacques Dubochet<sup>c</sup>, Axel Nemetz<sup>d</sup>, Wolfgang Knoll<sup>d</sup>, Horst Vogel<sup>a</sup>

<sup>a</sup> *Institut de Chimie Physique 4, Département de Chimie, Swiss Federal Institute of Technology, CH-1015 Lausanne, Switzerland*

<sup>b</sup> *Institut de Chimie Physique 2, Swiss Federal Institute of Technology, CH-1015 Lausanne, Switzerland*

<sup>c</sup> *Laboratoire d'Analyse Ultrastructurale, Bat. de Biologie, University of Lausanne, CH-1015 Lausanne, Switzerland*

<sup>d</sup> *Max-Planck-Institut für Polymersforschung, Ackermannweg 10, D-55128 Mainz, Germany*

Received 10 March 1995; in revised form 28 August 1995

## Abstract

In a recent paper, a new class of synthetic lipids, which self-assemble to form monolayers on gold surfaces, was introduced. The addition of a monolayer of phospholipids to these layers results in robust supported lipid bilayers designed to reconstitute transmembrane proteins. This paper presents a detailed characterisation of the monolayers and bilayers formed by these lipids and assesses their ability for the incorporation of membrane-spanning proteins. Film balance methods, electron microscopy, surface plasmon resonance, Fourier transform infrared measurements and Raman spectroscopy show the feasibility of this concept. However, further modifications to improve the thiolipids are necessary. A new strategy for the formation of laterally structured supported lipid bilayers is discussed and initial results are presented.

*Keywords:* Thiolipids; Supported lipid bilayers; Self-assembly; Biomimetic surfaces; Protein reconstitution; Surface patterning

## 1. Introduction

One of the most challenging issues in cell biology is the elucidation of the relationship between the structure and function of membrane-spanning proteins. These proteins play an essential role in the communication of cells with their environment, or, in the case of multicellular organisms, with neighbouring cells and the rest of the organism [1]. In general, the interaction between cell and information-carrying species (hormone, neuro-transmitter, photon) takes place at a membrane-spanning receptor protein which then triggers a biochemical cascade. Not only are these processes important for our understanding of cell biology, but, since many of these receptors are potential targets for pharmaceuticals, their investigation is also very important for the development of new drugs.

For a detailed scientific investigation of transmembrane proteins it is often necessary to reconstitute them under defined conditions [2]. One promising approach to the characterisation of such proteins is their incorporation into arti-

ficial lipid bilayers such as black lipid membranes (BLMs) or supported lipid bilayers. The electrochemical study of BLMs is already well established [3] but only allows investigation of the functional characteristics of channel-forming proteins and peptides. However, the deposition of membrane or lipid bilayer fragments containing membrane proteins onto solid surfaces has allowed the investigation of the morphology of transmembrane proteins using scanning probe microscopies [4,5] but has not yet provided direct access to the functional properties.

The controlled incorporation of proteins in active form into supported lipid bilayers should allow the use of the newly developed surface-sensitive techniques (scanning probe microscopies [6], optical evanescent wave methods [7]) and electrochemical techniques, thus enabling the study of the correlation between structure and function. The reconstitution of these proteins in supported lipid bilayers without the introduction of artefacts is, however, not necessarily straightforward because they are very delicate molecules that need a very specific environment to retain their activity.

Transmembrane proteins, as the name implies, consist of a hydrophobic region, which spans the lipid bilayer, and two

\* Corresponding author.

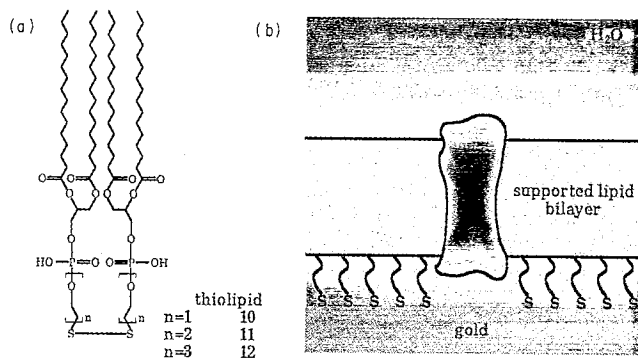


Fig. 1. (a) Structural formulae of the thiolipids. (b) Schematic representation of the proposed reconstitution of membrane-spanning proteins in a supported lipid bilayer covalently attached to a gold substrate. The hydrophilic spacer of the bound lipids decouples the bilayer from the solid substrate and allows the accommodation of hydrophilic extra-membraneous parts of the proteins in a suitably hydrated environment.

hydrophilic regions, which extend into the aqueous media on each side of the bilayer. Thus, to reconstitute transmembrane proteins and receptors in an environment similar to their natural one it is necessary to provide an aqueous environment on both sides of the bilayer which is sufficiently large to accommodate the extra-membraneous parts of the protein. In addition, the fluidity and composition of the lipid bilayer are critical for the correct functioning of the protein. Therefore, in order to create suitable artificial supported lipid bilayers, several exacting conditions must be fulfilled: the lipid layer must be maintained in a fluid state, which requires the structural decoupling of the 'soft' lipid layer from the rigid substrate surface in a few tens of ångströms while still maintaining a high layer stability; extra-membraneous parts of the proteins must be accommodated by conserving a thin water film between the lipid layer and the substrate; and finally, all interactions between the underlying substrate and the protein must be screened.

In an attempt to address these issues, we have introduced a new class of synthetic lipids ('thiolipids'), which were designed to create novel supported lipid bilayers on gold [8,9]. The structures of three thiolipids (**10**, **11**, **12**) are shown in Fig. 1(a): each thiolipid molecule consists of two phospholipid moieties, each attached to a hydrophilic spacer of variable length, and with the two halves of the molecule joined by a disulphide link at the ends of the spacers. These molecules are unusual in that they are both amphiphilic and contain a disulphide group which allows them to bind covalently to gold. Covalently bound monolayers of thiolipid on gold can be made by two methods: self-assembly of the thiolipids from detergent solution or LB transfer of a thiolipid monolayer from the air/water interface. The concept of the supported bilayers formed using these thiolipids is shown in Fig. 2(b): first a covalently bound monolayer of thiolipid is formed on the gold surface using the self-assembly technique [9]. The complete bilayer is then formed by immersing this surface in a solution of phospholipid vesicles. In a process

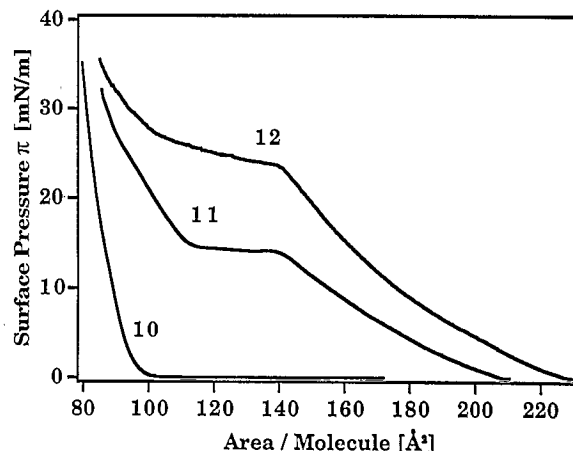


Fig. 2. Pressure-molecular area isotherms of thiolipids **10**, **11** and **12** (compression rate:  $3 \text{ \AA}^2 \text{ molecule}^{-1} \text{ min}^{-1}$ ; subphase: water; temperature:  $22^\circ\text{C}$ ).

driven by the hydrophobic interaction, these vesicles then self-assemble onto the hydrophobic thiolipid surface to form the second leaflet of the bilayer. The supported lipid layer thus formed has a number of advantages over the commonly used simple supported bilayers: first, the spacer acts as a buffer, decoupling the lipid layer from the solid surface; secondly, its hydrophilic nature ensures the provision of a hydrophilic environment between the lipid layer and the solid substrate.

Initial studies on the bilayers formed using these thiolipids have been very promising. In this paper we investigate in some detail to what extent such bilayers fulfil the exacting criteria necessary for the artifact-free reconstitution of membrane proteins. One important aspect is the similarity or otherwise of monolayers formed from thiolipids and from normal lipids found in cell membrane. To this end the phase behaviour of the thiolipids at the air/water interface was investigated and compared with that of conventional lipid systems. The structure of supported and LB transferred thiolipid layers was probed using a variety of techniques. Surface plasmon resonance (SPR) measurements allowed in situ monitoring of the formation of lipid layers on gold surfaces and gave the optical thicknesses of the layers. The physical state, the conformation and the orientation of the lipids were investigated using Raman spectroscopy and Fourier transform infrared (FTIR) measurements. Electron microscopy was used to probe the molecular order and phase structure of transferred monolayers. The ability of the hydrophilic spacer to decouple the lipid bilayer from the solid gold surface and to create a hydrophilic environment between the lipid layer and gold support was assessed by measuring the uptake of water into the layers in the hydrophilic atmosphere. Finally, we investigated the possibility of creating a more sophisticated laterally structured supported lipid bilayer based on thiolipids which overcomes some of the problems observed in the original bilayer systems.

## 2. Experimental details

The syntheses of the amphiphilic thiolipids **10**, **11** and **12** have been described in a previous publication [9]. 11-mercaptoundecanoic acid ( $\text{HS}(\text{CH}_2)_{10}\text{COOH}$ ) was synthesised using a new, simpler method. 4 g (0.015 mol) of 11-bromo-undecanoic acid ( $\text{Br}(\text{CH}_2)_{10}\text{COOH}$ ) was dissolved in 15 ml of ethanol. 2.3 g (0.03 mol) of thiourea in 10 ml of water were added to this. The mixture was refluxed for 3 h and then cooled in a refrigerator. The solid was filtered, washed with water and then dried under vacuum. The filtrate was evaporated to about half its original volume to recover a small quantity of second crop. The two crops were combined and added to 20 ml of water. 3 g of sodium hydroxide in 20 ml of water were added slowly to this suspension with stirring, until the reaction mixture became homogeneous. The mixture was refluxed for 3 h and cooled to room temperature. The reaction mixture was then acidified with conc.  $\text{H}_2\text{SO}_4$  and the white precipitate filtered, washed with water, and dried under vacuum (1.8 g). The compound was recrystallised from *n*-hexane. Proton NMR of the product in  $\text{CDCl}_3$  typically showed a quartet at 2.53, a triplet at 2.35 and the remaining methylene protons at 1.60 and 1.28 ppm relative to TMS, in agreement with the literature values [10,11]. 11-mercaptoundecanol was a generous gift from Dr. A. Ulman.

Palmitic acid (puriss.) and 1-palmitoyl-2-oleyl-*sn*-glycero-3-phosphocholine (POPC) (puriss.) were purchased from Fluka (Buchs, Switzerland). *N*-(7-nitrobenz-2-oxa-1,3-diazol-4-yl)-1,2-dimyristoyl-*sn*-glycero-3 phosphoethanolamine (NBD-PE) was purchased from Molecular Probes (Eugene, OR, USA).

Langmuir monolayers were prepared as described previously [12]. The lateral distribution of different phases (liquid, solid, etc.) of the monolayer at the air/water interface was studied using fluorescence microscopy. The different solubilities of a fluorescent probe (NBD-PE) in the different phases allows optimisation of the size and the distribution of the domains in the monolayers.

Substrates for film transfer or for self-assembly of thiolipid films were prepared by thermally evaporating gold films onto optical glass slides, as described in [12]. For Raman measurements silver-coated holographic gratings were used as substrates. The gratings were prepared as described in [13], vacuum-coated with silver and treated by plasma discharge immediately prior to transfer of the thiolipid film. Before spreading the molecules onto the water surface, the sample was dipped into the subphase.

Carbon-coated copper grids, rendered hydrophilic by glow-discharge in air, were used as substrates for TEM. Two grids were clamped back-to-back for the LB transfer, and thus one monolayer was deposited on each grid. A speed of approximately  $5 \mu\text{m s}^{-1}$  was used for the upstroke of the LB transfer. Images were obtained with a Philips CM12 electron microscope, operated at 80 kV. The low dose mode was used, with magnifications from  $2300\times$  to  $7500\times$ . The acceptable electron dose for recording an image was estimated from the

time the spots were visible under the beam. This was approximately 4 s, which corresponds to a dose of  $5 \text{e}^- \text{\AA}^{-2}$ . Negatives were developed in a Kodak D19 developer for 12 min at room temperature and printed on Agfa photographic paper grade 5. Dark field images were produced by replacing the objective aperture with a hexagonal fine bar copper grid, with the bars of the grid oriented so as to obscure the zero-order beam, while allowing the higher order diffracted beams to pass [14]. Bright field phase contrast images were recorded at a magnification of  $2300\times$  with a defocus of 1.1 mm.

The formation of self-assembled monolayers of thiolipid on gold was carried out in an aqueous medium (see [9] for more details). The lipid was solubilised in the form of small micelles in a solution of the detergent *n*-octyl- $\beta$ -D-glucopyranoside. The hydrophobic surface of the thiolipid monolayer was then used as a substrate for the formation of lipid bilayers. The preformed thiolipid monolayers were treated with an aqueous solution of the conventional lipid POPC in an *n*-octyl- $\beta$ -D-glucopyranoside solution which was diluted stepwise to below the critical micelle concentration (cmc) of the detergent.

For the preparation of the laterally structured monolayer templates the Langmuir–Blodgett transfer of the mixed monolayers to the gold substrates was executed at a speed of approximately  $5 \mu\text{m s}^{-1}$  during the up-stroke. After the film transfer, the samples were rinsed in ethanol and hexane to remove the palmitic acid, dried in an argon stream, and then immediately incubated for at least 12 h in a  $1 \text{mg ml}^{-1}$  solution of the appropriate sulphur-bearing molecules for the formation of self-assembly layers.

Transferred and self-assembled films were characterised using surface plasmon spectroscopy and surface plasmon microscopy [7,15]. These techniques allow both the determination of the optical thickness of the films and visualisation of small lateral thickness or refractive index variations. The optical thickness is a measure of the mass coverage per unit area. We used the Kretschmann coupling scheme [16]. The introduction of a simple lens and a CCD video camera into the scheme allowed microscopy of the film [17], with the surface plasmon resonance serving as a contrast mechanism.

Raman spectroscopy was used to investigate the molecular structure and ordering of the lipid monolayers. To overcome the intensity problems of supported ultra-thin film samples, surface plasmon enhanced Raman spectroscopy [18–20] was used, with the thiolipid monolayers transferred or self-assembled on silver-coated gratings [13].

FTIR measurements were performed using a Bomem Model 110 Michelson interferometer with the same configuration and ATR equipment as described in [21]. The molecular order parameter  $S_{\text{mol}}$  of the lipid chains was determined according to the method described in this paper. The dichroic ratio was derived from the C–H stretching vibrational bands applying a value of 0.5 for  $S_M$  ( $S_M$  describes the distribution of the transition moment  $M$  relative to the molecular director) and a value of 1.0 for  $S_m$  ( $S_m$  is the mosaic spread describing the distribution of the molecular axes to the layer normal).

### 3. Results

#### 3.1. Lipid monolayers at the air/water interface

The compression of monomolecular films of amphiphilic molecules at the air/water interface with simultaneous pressure reading (pressure vs. area isotherms) gives detailed information on the molecular dimensions, packing properties and phase transitions of the films [22]. Fluorescence microscopy allows observation of the lateral structure formation in the monolayer during phase transition [23–28]. The combination of these techniques represents one of the standard characterisations of amphiphilic molecules and, in this case, also provides a useful comparison with the phase behaviour of normal lipids.

The pressure vs. area/molecule isotherms of the three thiolipids are depicted in Fig. 2. While the isotherms of the thiolipids **11** and **12** show a clear discontinuity in the slope, indicating a first-order phase transition from a liquid-expanded to a solid-condensed state at approximately  $14 \text{ mN m}^{-1}$  and  $25 \text{ mN m}^{-1}$ , respectively, the isotherm of thiolipid **10** lacks this feature. There, from a flat region at  $\pi=0 \text{ mN m}^{-1}$  the curve rises steeply without an intermediate transition region. This establishes a clear monotonic dependence of the transition pressure of the film on the spacer length of the thiolipids, with the longest spacer giving the highest transition pressure. The areas per molecule at  $32 \text{ mN m}^{-1}$  of thiolipids

**10**, **11** and **12** are approximately  $80 \text{ \AA}^2$ ,  $85 \text{ \AA}^2$  and  $90 \text{ \AA}^2$ , respectively, which compares well with the area occupied by four extended hydrocarbon chains aligned along the normal to the water surface, or with two lipid molecules in the solid-analogous phase. All the films are extremely stable up to a pressure of  $40 \text{ mN m}^{-1}$  or higher for several hours.

The fluorescence micrographs of thiolipids **11** and **12** (Fig. 3) show dark, star-shaped domains, containing no fluorescent dopant, which emerge at the onset of the coexistence plateau of the phase transition, as in many conventional lipid systems [23–28]. The superstructures in which the domains arrange themselves are indicative of a repulsive interaction between the domains. While the domains are very regular for lipid **12**, the patterns of lipid **11** are much more irregular in shape and contain filamentous and dendrite-like elongations. Apparently, the length of the hydrophilic spacer group influences the pattern formation between the coexisting solid and fluid phases. During expansion, the patterns melt again and disappear completely at the discontinuity in the isotherms. The behaviour of the monolayers formed from thiolipid **10**, when observed under the fluorescence microscope, is quite different. Immediately on spreading the lipid solution at  $\pi=0 \text{ mN m}^{-1}$ , irregular structures appear. During compression, only the ratio between dark and bright areas increases, an effect which can be understood as a simple increase in the degree of crystallisation.

In summary, the thiolipids form Langmuir monolayers similar to those formed by conventional lipids at the air/water interface.

#### 3.2. Electron microscopy

Electron diffraction and microscopy allow determination of the molecular order and visualisation of the lateral structures in organic monolayers with molecular resolution. These techniques were used to investigate LB transferred monolayers of thiolipid **12**. The star-like domains observed at the air/water interface with fluorescence microscopy were imaged with both dark field and bright field phase contrast modes (Figs. 4(a) and (b)). Dark field microscopy images the domains with an estimated resolution of  $50 \text{ nm}$ . Several instances of brittle fracture of the stars can be observed. The fracture lines suggest that each point of the star is a separate subdomain. A darker central region is also observed in each star. Such subdomain structures have been observed recently in transferred thiolipid films using scanning force microscopy [29].

Phase contrast microscopy reveals the same star-like domain morphology. The low contrast between the solid and fluid phases made strong defocusing necessary. Thus the resolution is limited to approximately  $100 \text{ nm}$ . In this mode the electron microscope is highly sensitive to differences in material density, allowing localisation of single particles (e.g. proteins) with a molecular weight of  $5 \text{ kDa}$  or more. Such particles can be observed in the image as black spots surrounded by Fresnel rings. These particles are found either in

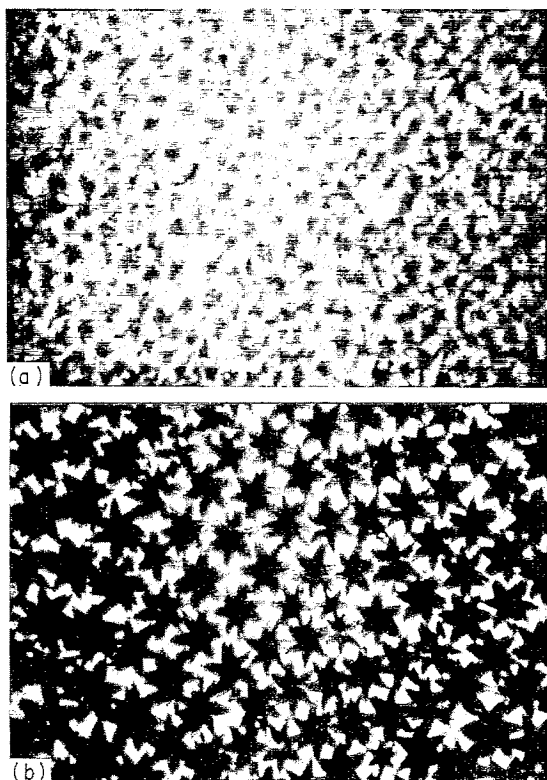


Fig. 3. Fluorescence micrographs of monolayers of thiolipid **11** (a) and thiolipid **12** (b) on the water surface at a surface pressure of  $30 \text{ mN m}^{-1}$  (well above the phase transition) at  $22^\circ\text{C}$ . The photographs show an area of  $120 \times 80 \text{ }\mu\text{m}^2$ .



Fig. 4. Electron micrographs of a monolayer of thiolipid **12** transferred in the coexistence region of the isotherm. (a) Dark field microscopy. The star-like 2D domains can easily be recognised. In the centre of the domains a darker region can be identified, probably indicating a less ordered phase. (b) Bright field phase contrast microscopy (defocus 1.1 mm). Small particles appear as dots and can be found either in the centre or at the borders of the star-like domains. The scale bar is 5  $\mu\text{m}$  in both cases.

the exact centre of a domain, at the edge of a domain or completely outside the domains, never within a subdomain. This suggests that many of the particles observed were present on the water surface where they acted as nucleation centres for the growth of the domains.

Finally, electron microscopy in the diffraction mode gives hexagonal diffraction patterns corresponding to a spacing of 4.4  $\text{\AA}$  between crystal axes, as previously reported for lipid layers [30,31].

### 3.3. Surface plasmon resonance

Surface plasmon resonance was used to monitor the self-assembly of thiolipid monolayers on gold surfaces and to characterise the completed monolayers. The adsorption of thiolipids onto the gold surface from the detergent solution took about 4 h after which no detectable change was observed. The angle shifts of the resonance minima of the different thiolipid SA films are summarised in Table 1. They are proportional to the optical thickness  $\Delta n \cdot d$  of the films ( $\Delta n$  is the refractive index difference between the organic film and the surrounding medium, and  $d$  is the geometrical thickness). The films consist of two monolayers: one chem-

Table 1  
0.1° of angle shift corresponds to a layer thickness of 6.4  $\text{\AA}$  (using a refractive index  $n = 1.45$ )

	Thiolipid layer		POPC layer
	$\Delta\theta$ (°) bilayer	$\Delta\theta$ (°) monolayer	$\Delta\theta$
Thiolipid <b>11</b>	$0.41 \pm 0.09$	$0.24 \pm 0.03$	$0.35 \pm 0.03$
Thiolipid <b>12</b>	$0.67 \pm 0.12$	$0.38 \pm 0.03$	$0.38 \pm 0.03$

isorbed to the gold substrate, the other, physisorbed, screening the hydrophobic hydrocarbon chains of the first layer from the solution. Table 1 also includes the shifts of the resonance angles after rinsing the film with an octylglucoside solution which removes the physisorbed monolayer, leaving only the covalently bound layer. The values are consistent with the formation of bilayers and monolayers, respectively. This characterisation has been described in more detail in a previous paper [9].

### 3.4. Raman measurements

Using Raman spectroscopy, we measured the ratio between the intensities of the bands of the symmetric  $\nu_s$  ( $\text{CH}_2$ ) stretching vibration at 2850  $\text{cm}^{-1}$  and the antisymmetric stretching band  $\nu_a$  ( $\text{CH}_2$ ) at 2880  $\text{cm}^{-1}$ . The relative intensities of these modes are sensitive to the intra- and intermolecular order of the hydrocarbon chains: the intensity ratio of the symmetric  $\nu_s$  ( $\text{CH}_2$ ) and the asymmetric  $\nu_a$  ( $\text{CH}_2$ )  $\text{CH}$ -stretching bands is used here as an empirical measure of the phase state and the conformational order of the lipid membranes [32–34]. Under our experimental conditions, the intensity ratio of the alkyl chains varies from 1.1 for crystalline samples to less than 0.7 for disordered chains.

In Fig. 5 the spectra of the  $\text{CH}$ -stretching region of thiolipids **11** and **12** are depicted for three different deposition techniques (LB transfer below the phase transition: A and D; LB transfer above the phase transition: B and E; self-assembly monolayers: C and F). For both thiolipids, the symmetric  $\nu_s$  ( $\text{CH}_2$ ) stretching vibration at 2850  $\text{cm}^{-1}$  is more prominent in the self-assembled monolayers. The asymmetric stretching band  $\nu_a$  ( $\text{CH}_2$ ) at 2880  $\text{cm}^{-1}$  is, in all LB-trans-

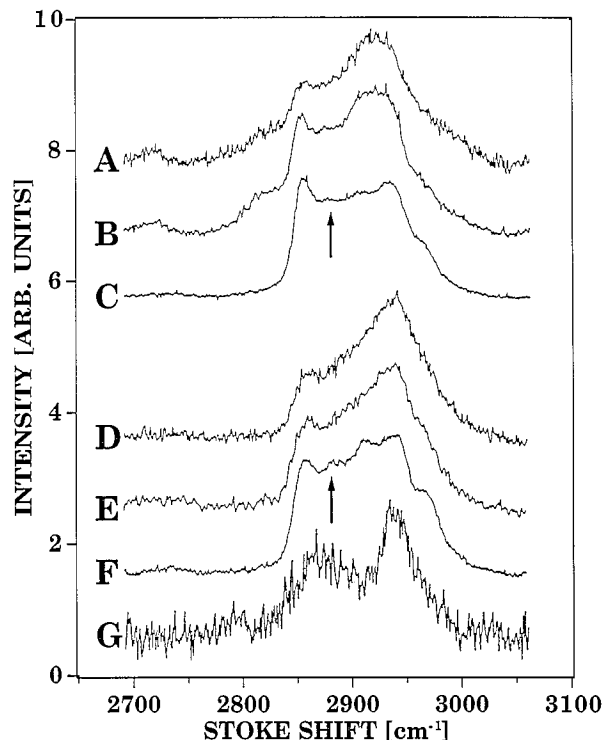


Fig. 5. Surface plasmon enhanced Raman spectra of the CH-stretching region taken from monolayers of thiolipid **11** (A–C) and **12** (D–F) and the spacer unit (g) on a thin silver film. Spectra a and d were taken from layers which were transferred by the LB technique below the phase transition ( $10 \text{ mN m}^{-1}$ ), B and E were taken from layers transferred by the LB technique above the phase transition ( $32 \text{ mN m}^{-1}$ ) and F and G were taken from self-assembly films.

ferred films, obscured by a broad band from  $2870$  to  $2970 \text{ cm}^{-1}$ . The  $\nu_a(\text{CH}_2)$  vibration can, however, be identified in the spectrum of the self-assembled films of thiolipids **11** and **12** (position indicated by arrows in Fig. 5). The very broad band is prominent in all cases, but the spectra taken from the self-assembly films allow the resolution of at least two bands at  $2910$  and  $2945 \text{ cm}^{-1}$ . As a reference, spectra were also recorded from the spacer unit ( $\text{SH}-\text{CH}_2-\text{CH}_2-\text{O}-\text{CH}_2-\text{CH}_2-\text{O}-\text{CH}_2-\text{CH}_3$ ). Two distinct bands can be identified at  $2870$  and  $2945 \text{ cm}^{-1}$ , respectively. The spectra taken from the fluid bulk phase of the spacer unit are identical to those of the self-assembled layers of the spacer on the silver surface.

Although it is difficult to assign all bands in the spectra and to obtain conclusive answers about the molecular order or to discover to what extent the hydrocarbon chains show an all-trans configuration, a few important conclusions can be drawn. Going from spectra A to C and from D to F for thiolipids **11** and **12**, respectively, a monotonic increase in the quality of the spectra is evident. If one assumes that the LB layers transferred from the condensed phase show a higher degree of chain order than those deposited from the fluid phase, extrapolation suggests that the spectra from the self-assembly layers possess the highest order.

The origin of the broad band between  $2870$  and  $2970 \text{ cm}^{-1}$  is not clear. It could be caused by varying contributions from the bands of the spacer units. A tilt of the spacer depending

on the chain order could account for this effect since the strongly polarised surface plasmon field (fixed in the lab coordinate system) interacts with the molecular scattering tensor elements according to their relative orientation. However, spectra recorded from alkylthiols of different chain length also show a broad featureless band in the same spectral region, which is normally assigned to various  $\text{CH}_3$  stretching modes [35]. For alkylthiols, this band becomes less prominent for longer hydrocarbon chains, and thus might be due to a variable orientation of the scattering tensor relative to the field polarisation.

Because of the broad obscuring band present on all spectra of the LB monolayers, the intensity ratios of the symmetric and antisymmetric stretching modes were only analysed for the spectra obtained from SA monolayers. The intensity ratio gives a value of  $0.82$  for thiolipid **11** and a value of  $0.96$  for thiolipid **12**. In identical experiments, SA monolayers of  $\text{HS}(\text{CH}_2)_{21}\text{OH}$ , which have their alkyl chains in a highly regular all-trans configuration, give an intensity ratio of  $0.82$ . Thus we conclude that the alkyl chains of the thiolipid are highly ordered, and that the lipid monolayers exist in the solid-analogous state.

### 3.5. Infrared spectroscopy

Infrared spectroscopy provides important information about the structure and orientational distribution of lipid molecules in supported layers, complementary to the information provided by Raman spectroscopy. Fig. 6 shows an ATR-FTIR spectrum of an LB-transferred monolayer of thiolipid **12** onto a germanium surface. The spectrum was taken with p-polarised excitation. The beam was incident at the coated crystal surface at an angle of  $45^\circ$ . In the spectral range between  $1000$  and  $2000 \text{ cm}^{-1}$ , three vibrational modes can

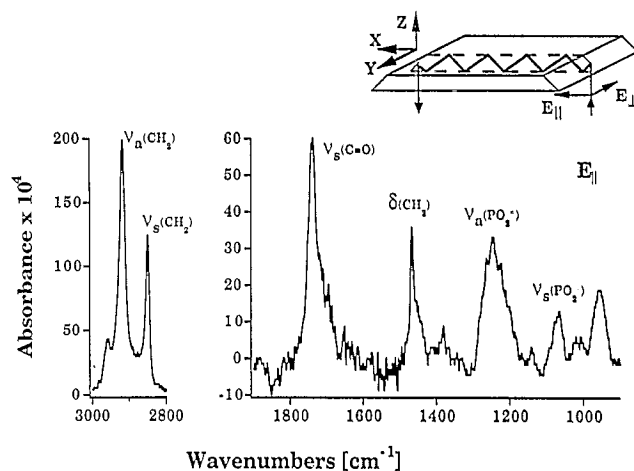


Fig. 6. FTIR spectrum of an LB monolayer of thiolipid **12** on a Ge-ATR crystal in the spectral regions between  $900$  and  $1800 \text{ cm}^{-1}$  and between  $2800$  and  $3000 \text{ cm}^{-1}$ . The spectrum was taken with p-polarisation ( $E_{\parallel}$ —see ATR schematic). The assignments of the most prominent bands are:  $1070 \text{ cm}^{-1}$ ,  $\text{PO}_2^-$  symmetric stretch;  $1250 \text{ cm}^{-1}$ ,  $\text{PO}_2^-$  antisymmetric stretch;  $1465 \text{ cm}^{-1}$ ,  $\text{CH}_2$  bending;  $1740 \text{ cm}^{-1}$ ,  $\text{C}=\text{O}$  symmetric stretch;  $2850 \text{ cm}^{-1}$ ,  $\text{CH}_2$  symmetric stretch;  $2920 \text{ cm}^{-1}$ ,  $\text{CH}_2$  antisymmetric stretch.

be assigned to the polar headgroup ( $\nu_s(\text{C}=\text{O})$ ,  $\nu_a(\text{PO}_2^-)$ , and  $\nu_s(\text{PO}_2^-)$ ) and one to the CH bending modes ( $\delta(\text{CH}_2)$ ). The low signal-to-noise ratio between 1600 and 1800  $\text{cm}^{-1}$  is due to baseline correction to correct for water bands. The most prominent bands of the spectrum are the symmetric and asymmetric  $\text{CH}_2$  stretching modes ( $\nu_s(\text{CH}_2)$ ,  $\nu_a(\text{CH}_2)$ ) which fall between 2800 and 3000  $\text{cm}^{-1}$ . By comparing this spectrum with reference spectra in the literature, we can be confident that the thiolipid hydrocarbon chains are in a crystalline-like state. In particular, the intensity ratio of the two  $\text{CH}_2$  stretching modes indicates an all-trans configuration of the hydrocarbon chains of the thiolipids. The single narrow band ( $\delta(\text{CH}_2)$ ) at 1470  $\text{cm}^{-1}$  indicates monoclinic packing of the hydrocarbon chains.

The orientational distribution of the molecular groups in the supported lipid layer can be characterised by the orientational order parameters which are obtained from the experimentally determined dichroic ratio  $R = A_{\parallel}/A_{\perp}$  (where  $A$  is absorbance) of polarised infrared measurements. The most suitable vibrational bands in this respect are the  $\text{CH}_2$  stretching vibrations at 2850 and 2940  $\text{cm}^{-1}$ . For a monolayer of thiolipid **12** we measured a dichroic ratio of  $R = 0.99$  which corresponds to an average orientational order parameter of the lipid chains of  $S_{\text{mol}} = 0.73$ . Assuming for a first approximation a single well-defined molecular tilt and not an orientational distribution of the all-trans hydrocarbon chains, the tilt angle can be calculated as  $\theta = 30^\circ$  ( $S_{\text{mol}} = \langle 3/2 \cos^2\theta - 1/2 \rangle$ ).

### 3.6. Swelling experiments

To study the role of the hydrophilic spacer of the thiolipids as a water-uptaking entity in a self-assembly monolayer, we performed swelling experiments [36,37], using surface plasmon resonance to monitor the thickness of the monolayer. The reflectivity was recorded as a function of time at an angle slightly lower than the resonance angle. Any shift in the resonance curve caused by adsorption to the gold surface resulted in a change in reflectivity. A gold substrate covered with a self-assembled monolayer of thiolipid **11** or **12**, respectively, was exposed to an atmosphere of 100% humidity and the thickness change was measured relative to the layer thickness in dry argon.

First a control experiment was performed with a monolayer of hexadecanethiol which self-assembles to give a layer of close-packed alkane chains, but does not contain any spacer units. In this case, no angle shift in the surface plasmon resonance occurred. The time-dependent response of the films of thiolipids **11** and **12** are shown in Fig. 7. It can clearly be seen that for both layers a thickness change takes place. If one compares the changes in reflectivity for both thiolipids and correlates them with water uptake (here using the simple model of a homogeneous layer of water) with a fitting routine based on the Fresnel equations and the known refractive index of water, a water film of thickness 1.2 Å for thiolipid **11** and 1.8 Å for thiolipid **12** was obtained. The reproducibility of

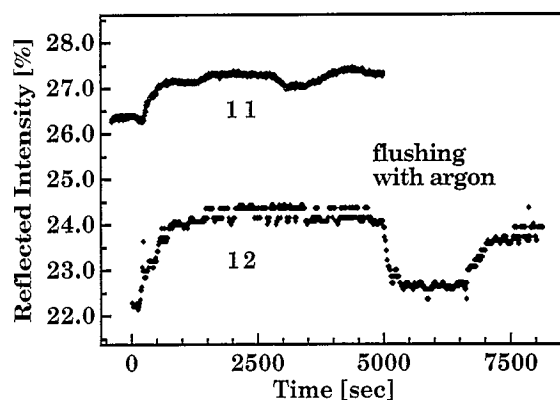


Fig. 7. Reflected intensity vs. time (SPR experiment) of monolayers of thiolipids **11** and **12** on exposure to 100% water vapour (the monolayers were in the presence of dry argon up to time  $t=0$ ). The reflected intensity was recorded at an angle slightly smaller than the resonance angle. The increase in the reflected intensity is due to a shift of the resonance curve.

these values is remarkable for both films and the fact that the ratio of thickness changes of both thiolipid layers correlates well with their respective numbers of ethoxy units forming the spacers makes it quite plausible to assume that the water take-up is due to the hydrophilic spacers. Although the calculated thicknesses of the postulated water layers are very small compared with the spacer lengths, it is clear that water can occupy only the excluded volume between the spacer groups. Furthermore, the response which is seen in this experiment gives no information about the absolute amount of hydration of the spacer region. It indicates only the reversible change of water take-up on going from a dry argon atmosphere to 100% humidity.

### 3.7. Mixed layers

To explore the formation of mixed bilayers (one leaflet of thiolipid, one leaflet of normal phospholipid), we investigated and compared the spontaneous formation of a second monolayer on a preformed thiolipid monolayer by self-assembly of phospholipids out of (i) detergent and (ii) vesicle dispersions [9,38,39]. With thiolipid **10**, no reproducible results were obtained. There, the assembled phospholipid layers could not be completely washed away with OG, which pointed to a possible intercalation of the phospholipids into the thiolipid film. Fig. 8 compares the time courses of the formation of POPC monolayers on a covalently bound thiolipid **12** monolayer using the two methods in water. The changes in reflectivity correspond to angle shifts of  $\Delta\theta = 0.38^\circ$  and  $\Delta\theta = 0.4^\circ$ . When the same experiments were performed in 0.1 M KCl solution the detergent method yielded similar results to those obtained in pure water, but the vesicle assembly procedure resulted in multilayer formation. For all thiolipid layers investigated, and for layers of 1-hexadecanethiol, the formation of a second layer of POPC resulted in angular shifts between  $0.3^\circ$  and  $0.4^\circ$ , i.e. on the average  $\Delta\theta \approx 0.35^\circ$ . These results are summarised in Table 1. Applying two refractive indices,  $n = 1.45$  and  $n = 1.5$ , as lower and

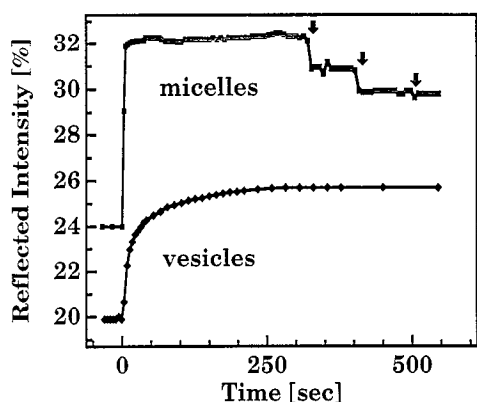


Fig. 8. Reflected intensity vs. time (SPR experiment) of a gold surface covered with a monolayer of thiolipid **12** on incubation (starting at time 0) with POPC in detergent solution (top curve) and in vesicle dispersion (bottom curve), respectively. Arrows indicate washing with 0.1 M KCl (see Section 2). The reflected intensity was recorded at an angle slightly smaller than the resonance angle.

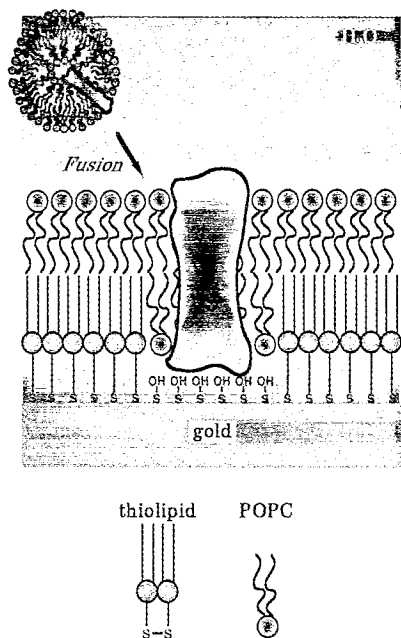


Fig. 9. The principle of reconstitution of membrane-spanning peptides and proteins in laterally structured supported lipid bilayers.

upper limits and using the appropriate SPR angle shifts, one can estimate a range of thicknesses for the phospholipid monolayer of 14–25 Å for POPC. Although there is some uncertainty in the accurate value of the thickness of the layers, the results are consistent with the formation of a single monolayer of phospholipid on the thiolipid-covered gold substrate.

### 3.8. Pattern formation

In the creation of supported lipid bilayers for the reconstitution of transmembrane proteins, a compromise between the properties required for the proteins (fluidity and flexibility of the membrane, appropriate hydrophobic and hydrophilic environments) and the mechanical properties of the whole

bilayer (stability, robustness) is necessary. One approach to this problem is to create structured lipid bilayers in which these different requirements are met in different well-defined regions. This concept is shown schematically in Fig. 9. In this figure the lipid layer contains two distinct types of regions: regions where one leaflet is a covalently bound thiolipid, and regions which are completely free-standing bilayers and which contain the reconstituted protein. With this goal in mind, we have developed a new technique to generate well-defined two-dimensional structures in thiolate films on gold. Here we describe this technique and demonstrate the feasibility of the approach.

The generation of a laterally structured thiol layer is depicted schematically in Fig. 10 and has been described in more detail in [12]. A mixture of palmitic acid and of thiolipid **12** is spread on the air/water interface of a Langmuir trough. On compression, the floating monolayer demixes to give regularly distributed domains, containing predominantly fatty acid. The size and shape of the domains depends on the self-organising properties of the monolayer and its manipu-

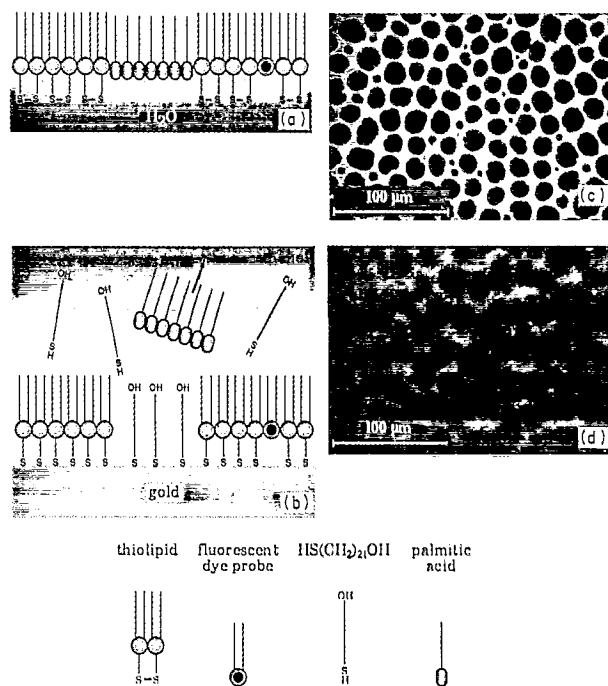


Fig. 10. Generation of a laterally structured thiolate layer. (a) shows a Langmuir film consisting of a mixture of palmitic acid and thiolipid at the air/water interface. In (b) the Langmuir monolayer has been transferred to a gold surface using the LB technique. After LB transfer the gold surface is washed in an appropriate solvent. The physisorbed palmitic acid domains are removed from the surface, while the thiolipid is not removed. Organic thiol molecules present in the solvent chemisorb to the newly exposed gold areas to form self-assembled monolayers. (c) and (d) show the corresponding experimental results. (c) Fluorescence micrograph of a mixed monolayer of thiolipid and palmitic acid with 1 mol% NBD-PE. The size and the shape of the domains are identical to those of a pure palmitic acid monolayer, indicating de-mixing of the components. (d) Surface plasmon micrograph of the corresponding film on a gold substrate which was washed with organic solvents after Langmuir transfer (before the subsequent self-assembly step). The angle of incidence ( $32.1^\circ$ ) was tuned to excite surface plasmon waves on the bare gold surface. The bare gold domains, therefore, appear dark.

lation on the Langmuir trough. The film is LB-transferred onto a gold substrate where the thiolipids bind covalently to the surface. The physisorbed fatty acid is washed away with a suitable solvent to leave domains of bare gold. A thiol monolayer is formed in these domains in a subsequent self-assembly step to give surface properties which contrast with the areas covered by the thiolipids.

In Fig. 10(c) a fluorescence micrograph of 4:1 mixed monolayer of palmitic acid and thiolipid **12** containing 1 mol% of a fluorescence labeled phospholipid is shown. The condensed domains are similar to those obtained from pure palmitic acid monolayers and the area occupied by the domains (at a given surface pressure) varies with the palmitic acid content of the film. We therefore conclude that the domains contain predominantly palmitic acid. This is confirmed by examining the surface plasmon micrograph (Fig. 10(d)) of a similar monolayer, transferred by the Langmuir–Blodgett technique onto a gold substrate and then rinsed in hexane and ethanol. The angle of incidence of the laser beam is tuned so that surface plasmons are excited only on the pure gold surface. No light is reflected from these regions and they appear dark. Analysis of the grey values of a sequence of micrographs taken at different angles allows determination of the local resonance angles. It shows that the dark domains in the lower part are bare gold patches. Their size and distribution correlate well with the domains on the floating monolayer.

### 3.8.1. Wetting experiments

The structured thiol layers can be used to create surfaces with patterns of contrasting wetting properties. For this purpose a self-assembled layer of 11-mercaptopundecanoic acid is formed in the bare gold patches: after washing the transferred layer, the substrate is immersed in a solution of 11-mercaptopundecanoic acid to form a monolayer. The contrasting wetting behaviour of this structured surface can be demonstrated by exposure to air saturated with ethanol vapour. The surface plasmon micrographs in Fig. 11 show such an experiment. In Fig. 11(a), in a dry atmosphere, little contrast is visible because there is little difference in thickness between the two layers (thiolipid and mercaptopundecanoic). In Fig. 11(b), in a saturated ethanol atmosphere, a huge contrast can be seen, with very high reflectivity from the hydrophilic areas indicating a very thick adsorbed film. Since the brightness within the spots is not homogeneous, we conclude that small ethanol drops have formed on the exposed hydrophilic areas.

### 3.8.2. Structured lipid layers

The contrasting wetting properties described in the previous example can also be used to create a structured phospholipid layer. It has been shown that if a highly hydrophobic surface, consisting of long hydrocarbon chains, is brought into contact with an aqueous solution containing phospholipid vesicles, the vesicles spontaneously fuse to the surface and form a lipid *monolayer* [9,38–40]. If the temperature of

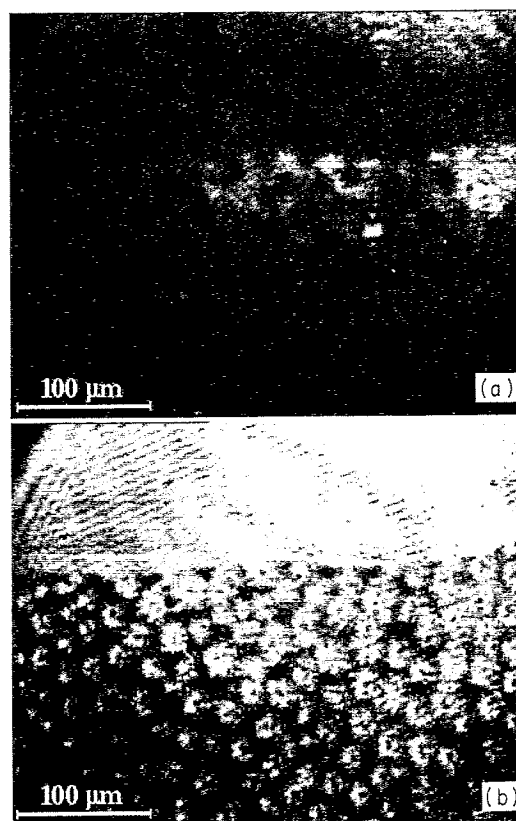


Fig. 11. Surface plasmon micrographs of a wetting experiment. (a) shows a micrograph of a LB-transferred film on gold. After transfer the film was washed, and a layer of  $\omega$ -mercaptopundecanoic acid was formed on the bare gold surfaces. There is little contrast in the micrograph, because the thicknesses of the thiolipid monolayer and the  $\omega$ -mercaptopundecanoic acid layers are similar. The horizontal line near the top of the picture is the limit of LB transfer and below this line the slightly paler, thicker thiolipid layer with darker domains can be seen. On exposure to air saturated with ethanol vapour, (b) was obtained. The previously dark domains and upper half of the sample have become bright, indicating a large change in the thickness of the adsorbed layer. On exposure to dry air, the effect is reversed. It is attributed to adsorption of ethanol to the hydrophilic areas of the surface.

the vesicle dispersion is above the phase transition temperature, a well-defined single monolayer is formed. In contrast, if a surface presents densely arranged hydroxyl groups, the exposure of such a surface to vesicle dispersion leads to the formation of a well-defined supported phospholipid *bilayer* [41]. We have exploited these effects to form a structured phospholipid layer containing well-defined regions of a monolayer and a bilayer.

Fig. 12(a) shows a surface plasmon micrograph of a patterned thiolate film on gold. It was prepared as described in the previous section. However, for the self-assembly step, a hydroxyl thiol (11-mercaptopundecanol) was used instead of a carboxythiol. No contrast can be seen in the image, since the film thicknesses of the thiolipid layer and the hydroxyl thiol layer are almost identical. This film serves as a template for the formation of the phospholipid layer. Figs. 12(b) and 12(c) consist of two surface plasmon micrographs of exactly the same area of the sample as shown in Fig. 12(a) (note the white spot, which is probably caused by a dust particle), but after immersing the substrate in an aqueous vesicle solution.

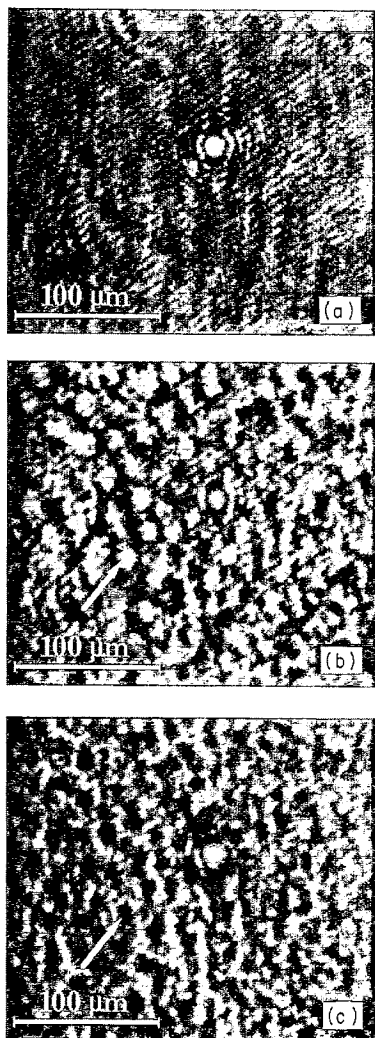


Fig. 12. Surface plasmon micrographs of a laterally structured layer of thiolipid and a long-chain hydroxythiol at the water–gold interface before (a), and after, (b) and (c), immersion in a POPC vesicle solution. The images are of exactly the same area (note the bright feature which is probably caused by a dust particle). No contrast can be seen in (a) owing to the match in thickness of the thiolipid and the hydroxyl thiol layer. In (b) and (c) a contrast is observed owing to the different spreading behaviour of the POPC vesicles on the hydrophobic and hydrophilic surfaces. Identical structures can be observed in (b) and (c), but micrograph (b) was taken at an angle of  $55.2^\circ$  and (c) was taken at  $56.2^\circ$ . These two angles produce a contrast inversion between the two images, so that the thicker domains appear bright in (b) and dark in (c). A typical domain is indicated in the two images with arrows.

In Fig. 12(b), the angle of incidence has been tuned so that surface plasmon modes are excited in the regions surrounding the domains ( $\theta = 55.2^\circ$ ; no light is reflected from these regions, therefore the domains appear bright), whereas in Fig. 12(c) the angle of incidence is slightly greater ( $\theta = 56.2^\circ$ ) in order to excite the surface plasmon modes within the domains (no light is reflected from the domains and they appear dark). From a detailed analysis of the grey values from a sequence of micrographs, the thickness changes on immersing the substrate in the vesicles have been determined. The domains became  $42 \text{ \AA}$  thicker, while the surrounding regions became  $22 \text{ \AA}$  thicker. These values correspond very

well to the formation of bilayers within the domains (expected thickness  $46 \text{ \AA}$ ) and of a monolayer for the remaining areas (expected thickness  $23 \text{ \AA}$ ). This experiment clearly demonstrates the potential of this technique for forming structured supported lipid layers as a matrix for the controlled reconstitution of membrane spanning peptides and proteins, as schematically shown in Fig. 9.

#### 4. Discussion

Our goal is the design of supported lipid membranes to accommodate membrane-spanning peptides and proteins. As already discussed in the introduction, this puts very stringent requirements on the design of these lipid layer systems. Here we discuss to what extent our present lipid layer system fulfils these requirements and what kind of modifications are likely to improve it.

Characterisation of the thiolipids on the Langmuir balance using pressure vs. area diagrams shows clearly that the thiolipids behave like a conventional lipid system as far as their thermodynamic properties are concerned. The phase transition behaviour is comparable with that of normal lipids, although the shape of the crystalline domains formed at the onset of the phase transition is rather unusual. Such shapes have recently been found in monolayers of long chain alcohols and esters [42–44]. At the moment it is unclear whether or not these similarities in domain structure reflect an underlying similarity between the thiolipid and alcohol/ester systems as distinct from other lipids. We note that the stability of the Langmuir monolayers of thiolipids is remarkable: at a pressure of  $40 \text{ mN m}^{-1}$  the film is stable for several hours.

Electron microscopy on transferred monolayers reveals a molecular ordering similar to that seen in comparable lipid monolayers. The domain structure at the air/water interface can clearly be seen to be conserved, an important point for the creation of structured lipid layers using combined LB and SA techniques. The visualisation of relatively low molecular weight particles in thiolipid monolayers using phase contrast electron microscopy is very promising for the investigation of peptide and protein incorporation in such monolayers.

Self-assembled monolayers of thiolipids on gold can be formed with the same ease as other monolayers of sulphur-bearing long chain molecules. Surface plasmon resonance measurements of the self-assembled monolayers give optical thicknesses which are consistent with a monolayer of lipids on the surface of the gold, although the relative differences in the optical thicknesses of the various thiolipid films are more pronounced than one would expect from the differences in the lengths of the different hydrophilic spacers. These differences in thickness may be explained by the dependence of the molecular packing of the thiolipid films on the length of the spacer units, with the longer spacers giving better packed films. It is probable that monolayers of the complex thiolipid molecules do not possess a close-packed structure commensurate with the underlying gold lattice. Thus, a rel-

atively long spacer may be necessary to decouple the thiolipid molecules from the gold surface and allow close packing of the alkyl chains.

A very important aspect of the supported lipid layers described in this paper is the formation of the second lipid monolayer (second leaflet) by physisorption to the hydrophobic thiolipid surface. The physisorption is a self-assembly process using normal phospholipids in a vesicle suspension, and is driven by the hydrophobic interaction: the addition of a monolayer of amphiphilic phospholipids to the surface screens the hydrophobic hydrocarbon chains of the thiolipid layer from the water. The importance of this step is in the use of vesicles for the self-assembly: membrane-spanning proteins may be incorporated into the vesicles during their formation and they can then act as 'shuttles' for the proteins. Several groups have demonstrated that this phospholipid self-assembly technique produces compact, insulating monolayers when the lipid system is in the fluid state [9,38–40]. There may be strong similarities between this process and the spreading of lipids at the air/water interface.

Investigation of the ordering of the thiolipid layer with infrared and Raman spectroscopy indicates that the hydrocarbon chains are in a closely packed all-trans configuration tilted at an angle of about 30° to the membrane normal. This conformation is unsuitable for the incorporation of proteins, since protein activity usually depends on membrane fluidity. To circumvent this problem modifications of the thiolipid structure can be introduced, e.g. increasing the length of the spacer unit, and thus improving the decoupling from the solid surface, or introduction of unsaturated carbon chains to favour lateral disorder in the thiolipid layer. To what extent the phase of the resulting film will resemble a 'real' fluid phase of a free lipid bilayer is uncertain, since the thiolipids will still be covalently bound to the support and therefore physically constrained. An alternative strategy is to structure the thiolipid layer and include small domains of free-standing phospholipid bilayer as described in the last section of the paper.

Another important aspect of the supported lipid layers is the inclusion of a hydrophilic region between the lipid bilayer and the substrate to accommodate the extramembraneous parts of the proteins. We have attempted to create such an environment by using spacers of ethylene oxide moieties for the thiolipids. Oligomers and polymers of ethylene oxide have been shown to be highly water soluble and are commonly used as moieties in protein-solubilising detergents. The hydrophilicity of the resulting layer between lipids and substrate was estimated by measuring the uptake of water by the thiolipid layers. A small reversible uptake of water was observed. However, the experiments described here are only able to measure changes in the water content of the thiolipid films and do not reveal anything about the absolute water content of the film in an aqueous environment. In addition, both the influence of the gold surface on the water uptake and the phase state of the water in the spacer layer are unknown.

In the final section of the results we have described a new strategy for the creation of supported lipid bilayers and our initial experiments in this direction. In our opinion, the generation of laterally structured thiolate monolayers opens up a promising route for the controlled reconstitution of membrane-spanning peptides and proteins in supported lipid bilayers. This technique should allow the creation of supported lipid layers in which certain areas are covalently bound to the substrate surface, while others are completely free-standing, as shown schematically in Fig. 9. Thus the robustness and stability of the layer are ensured by the bound areas of the thiolipids, while the fluidity and composition of the free-standing bilayers can be optimised separately. The use of a hydrophilic self-assembled monolayer in the domains between the thiolipids (e.g. a short chain hydroxythiol) screens the protein from detrimental interactions with the gold substrate and creates a hydrophilic environment between the two. Finally, since the lateral structures are formed by self-organisation, the lower limit on the size of the structures which can be created is on the molecular scale. Thus tiny cavities accommodating a single protein surrounded by an appropriate number of lipid molecules could be created.

## 5. Conclusions

We have presented a detailed study of a new class of synthetic lipids designed to fabricate supported lipid bilayers for the reconstitution of transmembrane proteins. Our results indicate that these new lipids allow the easy formation of lipid layers which fulfil, in many respects, the criteria we have set. However, it is clear that further studies and some modifications to the thiolipids are necessary. In particular, the phase state of the self-assembled thiolipid monolayers is not appropriate for the reconstitution of membrane proteins and the exact nature of the spacer layer (hydrophilicity, hydration) between the lipid moiety and the gold surface is not clear. Two approaches to the improvement of the lipid layers are currently in progress in our group: first, a new thiolipid has been synthesised, with a longer spacer and unsaturated lipid moieties, to increase disorder in the self-assembled monolayer. Secondly, a new strategy for the formation of laterally structured supported lipid bilayers has been adopted. This strategy should allow the formation of small areas of a free-standing lipid bilayer whose composition and fluidity can be optimised independently of the thiolipid structure.

## Acknowledgements

This work was supported financially by grants from the EPFL, the Roche Research Foundation, the European Institute of Technology (project B173) and the Swiss National Science Foundation (Priority Programme Biotechnology, project 5002-35180) to H.V.

## References

- [1] *Cold Spring Harbor Symposia on Quantitative Biology*, Vol. LVII, Cold Spring Harbor Laboratory Press, 1992.
- [2] O.T. Jones, J.P. Ernest and M.G. McNamee, in J.B.C. Findlay and W.H. Evans (eds.), *Biological Membranes: A Practical Approach*, IRL Press, 1987, pp. 139.
- [3] W. Hanke and W.-R. Schlue, *Planar Lipid Bilayers*, Academic Press, London, 1993.
- [4] K.N. Goldie, N. Panté, A. Engel and U. Aebi, *J. Vac. Sci. Technol. B*, 12 (1994) 1482.
- [5] F.A. Schabert, J.H. Hoh, S. Karrasch, A. Hefti and A. Engel, *J. Vac. Sci. Technol. B*, 12 (1994) 1504.
- [6] D.A. Bonnell (ed.), *Scanning Tunneling Microscopy and Spectroscopy*, Verlag Chemie, Weinheim, Germany, 1993.
- [7] W. Knoll, *MRS Bull.*, XVI (1991) 29.
- [8] H. Lang, C. Duschl, M. Grätzel and H. Vogel, *Thin Solid Films*, 210/211 (1992) 818.
- [9] H. Lang, C. Duschl and H. Vogel, *Langmuir*, 10 (1994) 197.
- [10] C.D. Bain, E.B. Troughton, Y.-T. Tao, J. EYall, G.M. Whitesides and R.G. Nuzzo, *J. Am. Chem. Soc.*, 111 (1989) 321.
- [11] H.D. Finklea and D.D. Hanshaw, *J. Electroanal. Chem.*, 347 (1993) 327.
- [12] C. Duschl, M. Liley and H. Vogel, *Angew. Chem. Int. Ed. Engl.*, 33 (1994) 1274.
- [13] A. Nemetz, T. Fischer, A. Ulman and W. Knoll, *J. Chem. Phys.*, 98 (1993) 5912.
- [14] H. Stahlberg, C. Duschl, M. Liley, H. Vogel and J. Dubochet, in *13th International Congress on Electron Microscopy*, Paris, 1994, pp. 971.
- [15] H. Raether, in G. Hass, M.H. Francombe and R.W. Hoffmann (eds.), *Physics of Thin Films*, Vol. 9, Academic Press, New York, 1977, pp. 145.
- [16] E. Kretschmann, *Opt. Commun.*, 6 (1972) 185.
- [17] B. Rothenhäusler and W. Knoll, *Nature*, 332 (1988) 615.
- [18] W. Knoll, M.R. Philpott, J.D. Swalen and A. Giraldo, *J. Chem. Phys.*, 77 (1982) 2254.
- [19] C. Duschl and W. Knoll, *J. Chem. Phys.*, 88 (1988) 4062.
- [20] H. Knobloch, C. Duschl and W. Knoll, *J. Chem. Phys.*, 91 (1989) 3810.
- [21] E. Thiaudère, M. Soekarjo, E. Kuchinka, A. Kuhn and H. Vogel, *Biochemistry*, 32 (1993) 12186.
- [22] A.W. Adamson, *Physical Chemistry of Surfaces*, Wiley, New York, 1976.
- [23] R. Peters and K. Beck, *Proc. Natl. Acad. Sci. USA*, 80 (1983) 7183.
- [24] M. Lösche, E. Sackmann and H. Möhwald, *Ber. Bunsenges. Physik. Chem.*, 87 (1983) 848.
- [25] H.M. McConnell, L.K. Tamm and R.M. Weis, *Proc. Natl. Acad. Sci. USA*, 81 (1984) 3249.
- [26] C.M. Knobler, *Science*, 249 (1990) 870.
- [27] H. Möhwald, *Ann. Rev. Phys. Chem.*, 41 (1990) 441.
- [28] H.M. McConnell, *Ann. Rev. Phys. Chem.*, 42 (1991) 171.
- [29] L. Santesson, T.W.H. Wong, M. Taborelli, P. Descouts, M. Liley, C. Duschl and H. Vogel, *J. Phys. Chem.*, 99 (1994) 1038.
- [30] A. Fischer and E. Sackmann, *Nature*, 313 (1985) 299.
- [31] I. Weissbuch, J. Majewski, L. Margulis, M. Lahav and L. Leiserowitz, *J. Phys. Chem.*, 97 (1993) 8692.
- [32] B.P. Gaber and W.L. Peticolas, *Biochim. Biophys. Acta*, 465 (1977) 260.
- [33] R.G. Snyder, S.L. Hsu and S. Krimm, *Spectrochim. Acta, A*, 34 (1978) 395.
- [34] M. Harrand, *J. Chem. Phys.*, 79 (1983) 5639.
- [35] M.A. Bryant and J.E. Pemberton, *J. Am. Chem. Soc.*, 113 (1991) 3629.
- [36] Y.L.E. Chen, M.L. Gee, C.A. Helm, J.N. Israelachvili and P.M. McGuiggan, *J. Phys. Chem.*, 93 (1989) 7057.
- [37] Y.L. Chen, C.A. Helm and J.N. Israelachvili, *Langmuir*, 7 (1991) 2695.
- [38] J. Spinke, J. Yang, M. Liley, H. Ringsdorf and W. Knoll, *Biophys. J.*, 63 (1992) 1667.
- [39] S. Terretaz, T. Stora, C. Duschl and H. Vogel, *Langmuir*, 9 (1993) 1361.
- [40] E. Kalb, S. Frey and L.K. Tamm, *Biochim. Biophys. Acta*, 1103 (1992) 307.
- [41] C. Duschl, unpublished results.
- [42] C.M. Knobler, *Ann. Rev. Phys. Chem.*, 43 (1992) 207.
- [43] X. Qiu, J. Ruiz-Garcia, K.J. Stine, C.M. Knobler and J.V. Seliger, *Phys. Rev. Lett.*, 67 (1991) 703.
- [44] S. Hénon and J. Meunier, *J. Chem. Phys.*, 98 (1993) 9148.